pH-Responsive Polyelectrolyte Coatings that Enable Catheter-Mediated Transfer of DNA to the Arterial Wall in Short and Clinically Relevant Inflation Times

Yan Yu,[1,†] Visham Appadoo,[2,†] Jun Ren,[3] Timothy A. Hacker,[4,*] Bo Liu,[3,*] David M. Lynn[1,2,*]

[1]*Department of Chemical and Biological Engineering, University of Wisconsin-Madison, 1415 Engineering Drive, Madison, Wisconsin 53706, USA;* [2]*Department of Chemistry, University of Wisconsin–Madison, 1101 University Ave., Madison, WI 53706, USA;* [3]*Division of Vascular Surgery, Department of Surgery, University of Wisconsin – Madison, 1111 Highland Avenue, Madison, Wisconsin 53705;* [4]*Cardiovascular Research Center, University of Wisconsin–Madison,* 600 Highland Ave., Madison, WI 53792, *USA;* [†]*Equally contributing author; Email: (D.M.L.) dlynn@engr.wisc.edu*

ABSTRACT: We report the design and characterization of pH-responsive polymer coatings that enable catheter balloon-mediated transfer of DNA to arterial tissue in short, clinically relevant inflation times. Our approach exploits the pH-dependent ionization of poly(acrylic acid) (PAA) to promote disassembly and release of plasmid DNA from polyelectrolyte multilayers. We characterized the contact-transfer of multilayers comprised of PAA, plasmid DNA, and linear poly(ethyleneimine) (LPEI) identified as promising in prior studies on the delivery of DNA to arterial tissue. In contrast to thinner films evaluated previously, we found thicker coatings comprised of 32 repeating $(LPEI/PAA/LPEI/DNA)_x$ tetralayers to swell substantially in physiologically relevant media (in PBS; pH = 7.4). In some cases, these coatings also disintegrated or delaminated rapidly from their underlying substrates, suggesting the potential for enhanced balloon-mediated transfer. We developed a technically straightforward agarose gel-based hole-insertion model to characterize factors (inflation time, lumen size, etc.) that influence contact transfer of DNA when film-coated balloons are inflated into contact with soft surfaces. Those studies and the results of *in vivo* experiments using small animal (rat) and large animal (pig) models of peripheral arterial injury revealed catheters coated with these materials to promote robust contact transfer of DNA to soft hydrogel surfaces and the luminal surfaces of arterial tissue using inflation times as short as 30 seconds. These short inflation times are relevant in the context of clinical vascular interventions in peripheral arteries. Additional studies demonstrated that contact transfer of DNA using these short times can promote subsequent dissemination and transport of DNA to the medial tissue layer, suggesting the potential for use in therapeutically relevant applications of balloon-mediated gene transfer.

Keywords: polymers, thin films, coatings, contact transfer, DNA

For Table of Contents Use Only:

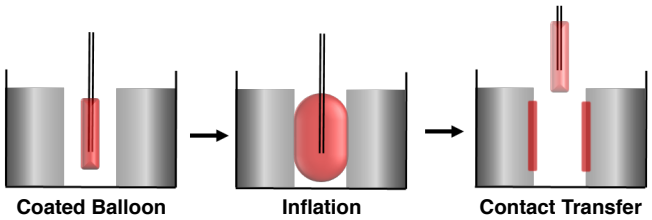

Introduction

Thin polymer-based films fabricated by the layer-by-layer assembly of oppositely charged polymers (known as 'polyelectrolyte multilayers', or PEMS) have attracted significant interest in many fundamental and applied biomedical and biotechnological contexts owing, in part, to their compositional complexity and the ease with which they can be applied to the surfaces of complex objects.[1-13] The mild aqueous conditions that are often used for the assembly of these materials can preserve the bioactivities of nucleic acids and proteins, rendering this approach particularly attractive for the design of coatings comprised of bioactive agents.[3, 14-25] The iterative nature of layer-by-layer assembly can also provide opportunities to manipulate structure and composition at the nanoscale or incorporate design elements that are useful for the subsequent controlled release or local delivery of macromolecular drugs.[26-36] The work reported here was motivated broadly by potential applications of PEMs as platforms for the local delivery of DNA during vascular interventions and, in particular, by key challenges associated with the design of coatings that can promote the rapid and uniform 'contact transfer' of DNA to vascular tissue from the surfaces of interventional devices used during minimally-invasive surgeries.

Our group[37-42] and others[43-55] have previously reported on strategies to promote the release of transcriptionally active DNA from surfaces coated with PEMs. These strategies have generally focused on the design of multilayers that erode, disassemble, or deconstruct in aqueous environments promoted, at least in part, by the chemical degradation of their polymeric building blocks. For example, cationic polymers that are hydrolytically,[37, 39, 42, 48, 56, 57] reductively,[45-47, 58, 59] or enzymatically[44] degradable have been used to tune film disassembly and promote the sustained, surface-mediated release of DNA over periods ranging from days to weeks or

months.[26, 39, 56, 57] In contrast, there are fewer reports describing approaches useful for the release or delivery of DNA on shorter time scales (e.g., over periods of a few seconds or a few minutes).[50, 55, 60-62] In the context of potential applications in clinical interventions, another significant and related challenge lies in designing PEMs that can be transferred rapidly and faithfully from one surface to a second target surface (e.g., by temporarily pressing a coated device into contact with soft tissue).[63, 64] Materials that promote the contact transfer of DNA onto other soft surfaces could provide new tools for basic biomedical research and could also enable new approaches to localized gene-based therapies. The degree of control over physicochemical and temporal factors that influence the levels of film stability—and instability—required for effective contact transfer differs substantially from that required for the design of PEMs that simply disintegrate and release their contents into solution.

We previously reported on a strategy for the design of DNA-containing PEMs that addresses some of the challenges noted above and enables the contact transfer of DNA to other surfaces.[60, 62] That approach exploited phenomena arising from pH-dependent ionization of a weak polyelectrolyte, poly(acrylic acid) (PAA), in multilayers fabricated from PAA, plasmid DNA, and the cationic polymer linear poly(ethyleneimine) (LPEI). PEMs fabricated from these components in a repeating "tetralayer" structure [e.g., $(LPEI/PAA/LPEI/DNA)_x$] eroded, disintegrated, and released transcriptionally active DNA rapidly upon incubation in aqueous media at physiologically relevant pH (e.g., in PBS; pH = 7.4). We also demonstrated that this 'weak polyelectrolyte approach' could be used to fabricate uniform coatings on inflatable balloon catheters and promote the contact transfer and localized expression of plasmid DNA *in vivo* using a rat model of vascular injury.[62] In those experiments, we used balloons coated with

plasmid DNA encoding a reporter gene and balloon inflation times of 20 minutes to increase the likelihood of transfer and gene expression.

This study sought to further characterize the physicochemical behaviors of LPEI/PAA/LPEI/DNA-based coatings and develop approaches useful for the rapid, balloon-based contact transfer of DNA on substantially shorter and clinically relevant time scales. As part of these efforts, we also developed a technically straightforward agarose gel-based 'hole-insertion' model that can be used to characterize factors that influence the contact-mediated transfer of DNA to adjacent soft surfaces when film-coated balloon catheters are inflated into contact. The results of those model studies and the results of subsequent *in vivo* experiments using small animal (rat) and large animal (pig) models of peripheral arterial injury demonstrate that balloons coated with LPEI/PAA/LPEI/DNA films 32-tetralayers thick can promote robust contact transfer of plasmid DNA to soft hydrogel surfaces and the surfaces of soft arterial tissue using inflation times as short as 30 seconds. These times are substantially shorter than contact-transfer times reported in past studies on thinner LPEI/PAA/DNA coatings (20 minutes), and are relevant in the context of clinical vascular interventions in peripheral arteries. These and other results arising from this study suggest the potential for use in therapeutically relevant applications of balloon-mediated gene transfer.

Materials and Methods

Materials. Linear poly(ethyleneimine) (LPEI, MW = 25,000) and poly(acrylic acid) (PAA, MW = 90,000) were purchased from Polysciences, Inc. (Warrington, PA). Plasmid DNA encoding luciferase (pCMV-Luc; 6201 b.p.) was purchased from Elim Biopharm (San Francisco, CA).

Fogarty arterial embolectomy catheters (2-French diameter) were purchased from Edwards Lifesciences, LLC (Irvine, CA). For experiments requiring fluorescently labeled DNA, a tetramethylrhodamine (TMR) Label-IT nucleic acid labeling kit was purchased from Mirus Bio Corporation (Madison, WI) and was used according to the manufacturer's instructions. Solutions of sodium acetate buffer (VWR, West Chester, PA) and phosphate-buffered saline (PBS; EM Science, Gibbstown, NJ) were prepared by diluting commercially available concentrate. All materials were used as received unless otherwise noted. Solutions of LPEI and PAA used to fabricate multilayers were filtered through a 0.2 μm nylon membrane syringe prior to use.

General Considerations. Sodium acetate buffer (100 mM, pH = 4.9) was used for all rinsing steps during film fabrication and the preparation of polymer and DNA solutions. Fluorescence microscopy and phase contrast microscopy images were acquired using either an Olympus IX70 fluorescence microscope, Nikon Eclipse E600, or a Ti-U Eclipse fluorescence microscope using Metavue 7.1.2.0, cellSens, or Nikon Elements software packages, respectively. Optical microscopy images were analyzed using ImageJ Software (NIH). The morphologies of coatings fabricated on the surfaces of catheter balloons were characterized using scanning electron microscopy (SEM) using a LEO SEM microscope in high-vacuum mode at 5 kV. The amount of DNA released from the multilayered films during incubation in PBS was quantified by recording UV-vis absorbance values at a wavelength of 260 nm (corresponding to the absorbance maximum of double-stranded DNA) using a DU 520 UV-vis spectrophotometer (Beckman Coulter, Fullerton, CA).

Preparation of Polyelectrolyte Solutions. Solutions of LPEI and PAA (5 mM with respect to the repeat unit molecular weight of the polymer) were prepared using 100 mM sodium acetate buffer (pH 4.9). Solutions of plasmid DNA were prepared at 1 mg/mL in 100 mM acetate buffer (pH 4.9) but were not filtered prior to use. For experiments requiring fluorescently labeled DNA, labeled DNA was added to a solution of unlabeled DNA to give labeled/unlabeled plasmid solutions of 5% (w/w) for *in vitro* experiments and 40% for *in vivo* experiments.

Fabrication of Multilayered Films on the Surfaces of Inflatable Catheter Balloons. Films were fabricated layer-by-layer on embolectomy catheter balloons using an automated dipping robot (Riegler & Kirstein GmbH, Potsdam, Germany) according to the following protocol: 1) the balloons were completely immersed in a solution of LPEI for 5 minutes, 2) the balloons were removed and immersed in two wash baths of 100 mM acetate buffer for one minute each, 3) the balloons were then immersed in a solution of anionic polymer (either PAA or DNA; as appropriate, see below) for 5 min, and (4) the balloons were rinsed again in the manner described above. Up to four balloons were coated simultaneously using this approach, and this cycle was repeated until the desired numbers of cationic and anionic polymer layers were deposited. This general procedure was used to fabricate films having the following general structure: $(LPEI/PAA/LPEI/DNA)_x$, where 'x' denotes the number of polymer 'tetralayers' deposited. After fabrication, film-coated balloons were rinsed with 18 MΩ deionized water, allowed to air dry following the final rinse step, and then stored in their original packaging in a dry, dark location prior to use. All films were fabricated and stored at ambient room temperature.

Characterization of Film Stability and DNA Release Profiles. Experiments designed to investigate film stability and characterize the release of DNA from multilayered films were performed in the following general manner. Film-coated inflatable embolectomy catheter balloons were submerged in PBS (1 mL, pH = 7.4, 137 mM NaCl) in plastic UV-transparent cuvettes. The cuvettes were sealed using parafilm, and the samples were incubated at 37 °C without agitation and removed at predetermined intervals for characterization and UV-vis spectroscopy. The concentration of DNA released from the films into solution over time was characterized by measuring the UV absorbance of the PBS incubation buffer (at a wavelength of 260 nm, the absorbance maximum of DNA). After each set of measurements, the coated substrates were placed into new cuvettes with fresh aliquots of PBS and returned to the incubator at 37 °C.

Characterization of Contact-Mediated Transfer of DNA Using an Agarose Gel Model. Agarose gels were prepared by dissolving agarose powder (Difco Agar Noble, Becton, Dickinson and Company, Sparks, MD, USA) in PBS buffer (pH = 7.4) at a concentration of 3% by mass.[65] The mixture was heated using a microwave until the agarose powder was completely dissolved. The resulting solution was cooled under running tap water and then poured into a polystyrene chamber (Nunc Lab-Tek II Chamber Slide System, Thermo Scientific, USA). A solid metal cylinder of known diameter (i.e., 2 mm, 3 mm, or 4 mm) was inserted during gel solidification and removed after the gel was completely solidified to create well-defined holes with sizes similar to those of arteries in rats and pigs used in our past studies.[41, 62] The gel was equilibrated to 37 °C prior to use. Film-coated catheter balloons were imaged using a

fluorescence microscope and then inserted vertically into the hole of the gel. The balloon was then inflated with ~2 mL of air until it expanded against the wall of the hole. After incubation for a defined period of time at 37 °C, the balloon was deflated, removed, dried under a stream of air for ~3 min and then imaged again using fluorescence microscopy. The fluorescence intensity of each balloon was then analyzed again using ImageJ software. After removal of the balloons, gel samples were collected, sliced horizontally and/or vertically, and the resulting cross-sections were imaged using fluorescence microscopy.

General Surgical Procedures. For experiments using rats: After induction of anesthesia with 2.5% isoflurane, arterial injury was induced in male Sprague-Dawley rats (~2-3 months old, ~350 g) by means of carotid balloon angioplasty as described previously.[66] Briefly, a longitudinal incision was made in the neck of the rat in order to isolate the left external, internal, and common carotid arteries. Three passages of an uncoated angioplasty balloon inflated to a pressure of 2 atm were then used to denude the common carotid artery of the endothelial layer. Next, a balloon coated with a LPEI/PAA/LPEI/DNA film (32 tetralayers thick, see below) was inserted and inflated until it was observed to expand against the arterial wall (~2 atm). After a 2-minute incubation period, the balloon was deflated and removed from the artery. The external carotid artery was then ligated, blood flow was restored to the common and internal carotid arteries, and the surgical wound was closed layer-to-layer. Animals were sacrificed post-operatively at a predetermined time depending on the timescale of the experiment (see below).

For experiments using pigs: Swine (25-30 kg) were pre-medicated with a drug cocktail composed of Telazol (4-6 mg/kg IM) and Xylazine (2 mg/kg, IM), intubated, and anesthetized

with isoflurane (1-5%). All animals were placed on a heating pad to prevent a drop in body temperature upon administration of anesthesia. A cut down to access the femoral artery was performed and 2-3 inches of artery was exposed and dissected free from the surrounding tissue. Vascular clamps were placed on the artery above and below the incision to control bleeding. A small cross-sectional cut was made in the artery and an uncoated angioplasty balloon was inflated to a pressure of 4-6 atm (depending on the size of the artery) and advanced and retracted 10 times to denude the artery of the endothelial layer. Next, a balloon coated with a LPEI/PAA/LPEI/DNA film (32 tetralayers thick, see below) was inserted and inflated until it was observed to expand against the arterial wall (4-6 atm). After a 30-second or 1-minute incubation period, the balloon was deflated and removed from the artery.

For studies designed to characterize initial DNA transfer, animals were sacrificed immediately and treated vessels were collected. For studies designed to characterize DNA dissemination over time, treated vessels were repaired with 10-0 proline and then the muscle and skin were closed in layers and the animal was recovered for 15 hours, at which time the animal was sacrificed and the vessels were collected for histology. All experimental protocols were approved by the Institute Animal Care and Use Committee at University of Wisconsin-Madison (#M02285 and #M01839) and conformed to the Guide for the Care and Use of Laboratory Animals published by the NIH Publication No. 85-23, 1996 revision.

Characterization of DNA Delivery and Dissemination in Rat and Pig Arteries. For experiments designed to characterize the extent of contact-transfer of DNA to rat and pig arterial tissue following balloon-mediated delivery, the artery (carotid for rats; femoral for pigs) was

treated with a balloon coated with a film having the structure (LPEI/PAA/LPEI/pCMV-Luc_{TMR})$_{32}$. Balloons were inflated for a pre-determined period of time (see text) and then deflated and removed. Animals were sacrificed either immediately or 15 hours after surgery, and film-treated arteries were embedded and frozen in OCT compound and cut into 5 μm sections for characterization by fluorescence microscopy.

Results and Discussion

Characterization of Film-Coated Balloon Catheters

Balloon catheters were coated with LPEI/PAA/LPEI/DNA films 32-tetralayers thick using a layer-by-layer fabrication procedure similar to our previous methods (see Materials and Methods for additional details).[62] Films having this general 32-tetralayer structure will be referred to from here on with the following notation: (LPEI/PAA/LPEI/DNA)$_{32}$. For physical characterization studies and most other studies described below, films were fabricated using a plasmid DNA construct (pCMV-Luc_{TMR}) encoding firefly luciferase and fluorescently labeled with the fluorophore tetramethylrhodamine (TMR) to permit characterization of film uniformity using fluorescence microscopy; past studies demonstrate that the balloon catheters used here do not exhibit confounding autofluorescence in the red (TMR) channel.[40] All experiments were performed using standard-sized 2-French balloon catheters.

Figure 1A shows a schematic illustration of a balloon catheter showing the selective fabrication of DNA-containing multilayers, shown in red, on the inflatable balloon. Figure 1C shows a low-magnification fluorescence microscopy image of a film-coated balloon. Inspection of this image reveals fluorescence to be distributed uniformly over the surface of the balloon. Figure 1B shows a higher magnification image of a portion of the film-coated balloon shown in

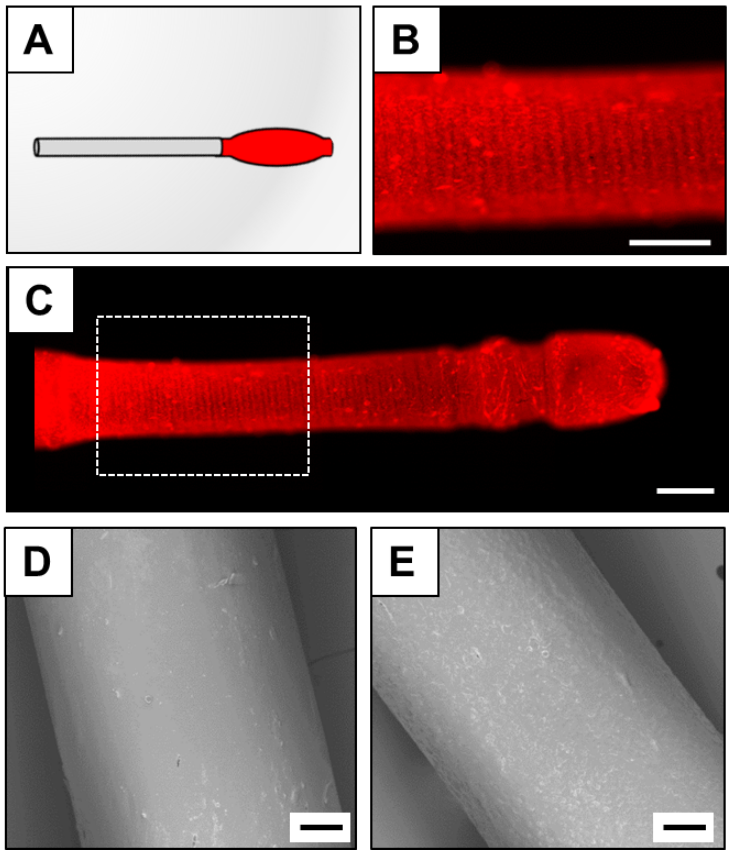

Figure 1: (A) Schematic showing a catheter balloon coated with a multilayer film (shown in red). (B, C) Fluorescence microscopy images of a balloon coated with a $(LPEI/PAA/LPEI/DNA)_{32}$ film fabricated using a plasmid labeled with the fluorophore TMR (red) at (B) high and (C) low magnification. The dashed box in (C) indicates the location of the portion of the film shown at higher magnification in (B). Scale bars in (B, C) are 500 μm. (D, E) SEM images of (D) a bare, uncoated balloon and (E) a balloon coated with a $(LPEI/PAA/LPEI/DNA)_{32}$ film. Scale bars in (D, E) are 100 μm.

Figure 1C to show additional detail. Further characterization of film morphology was performed using scanning electron microscopy (SEM). The panels in Figure 1D-E show SEM images of a portion of a bare (uncoated) balloon (Figure 1D) and a balloon coated with a 32-tetralayer LPEI/PAA/LPEI/DNA film (Figure 1E). Comparison of these images reveals (i) the presence of a uniform coating on the surface of the balloon (consistent with the fluorescence microscopy images) and (ii) that these 32-tetralayer films are relatively smooth and devoid of significant topographic features, similar to the surfaces of the bare, uncoated balloons.

Characterization of Film Stability and Release of DNA in Physiological Media

Our past studies demonstrated that LPEI/PAA/LPEI/DNA films up to 16 tetralayers thick fabricated on planar silicon substrates release DNA rapidly (with >65% of DNA released in the first five minutes) when incubated in physiologically relevant media (e.g., PBS; pH = 7.4; 37 °C).[62] To characterize the rates and extents of the release of DNA promoted by the thicker 32-bilayer films investigated here on the soft and flexible surfaces of the latex balloon catheters used here, we incubated uninflated balloons coated with $(LPEI/PAA/LPEI/DNA)_{32}$ films in PBS at 37 °C. The amount of DNA released as a function of time was monitored by both UV-Vis absorbance using films fabricated using non-labeled DNA (Figure 2A) and by fluorometry using films fabricated using DNA labeled with TMR, as described above (Figure 2B).

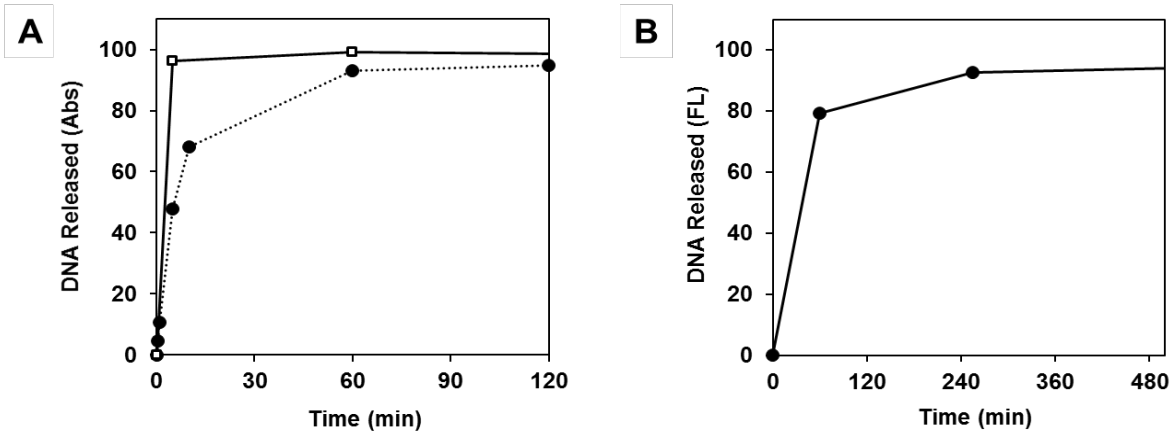

Figure 2: Plots of DNA released versus time for balloons coated with $(LPEI/PAA/LPEI/DNA)_{32}$ films incubated in PBS at 37 °C, as determined using UV-Vis absorbance (A) or fluorometry (B). Data represented by the open squares correspond to an experiment in which film delamination was observed to occur. DNA release is presented as percentages of the total DNA released from the balloons in each experiment.

The 32-tetralayer coatings used here were observed to swell substantially upon introduction to PBS, as determined by visual inspection. The release of DNA from the film-coated balloons into solution was generally fast in all cases, but we observed some variation in the rates of DNA release from experiment to experiment. In some cases, we observed large-scale film delamination and/or the rapid loss of large pieces of disintegrated coatings into surrounding buffer. In these cases, the release of DNA into solution occurred rapidly and nearly quantitatively (e.g., Figure 2A, open squares; when delamination and disintegration were observed, more than 95% of DNA was released within the first five minutes). In other cases, film delamination and disintegration was not observed. In these cases, DNA was released more gradually, with about 90% released over a period of about one to two hours [e.g., Figure 2A (solid circles) and Figure 2B].

The swelling and delamination of these 32-tetralayer coatings, and the subsequent rapid delamination observed in some cases, contrasts to the behaviors of the 16-tetralayer coatings characterized in past studies (which do release DNA rapidly, but were not observed to swell or delaminate substantially upon introduction to PBS).[62] The factors leading to differences in the observed behaviors of these films were not investigated further as part of this study. However, the observation that these 32-tetralayer films can swell and delaminate readily from their underlying balloon substrates prompted a series of additional studies, described below, to determine the potential utility of these coatings in the context of inflation-mediated contact transfer.

Characterization of Contact-Mediated Transfer of DNA to Secondary Surfaces Using an Agarose Gel Model

In view of the observations of film swelling and delamination discussed above, we reasoned that these 32-tetralayer films might be particularly well suited for the development of new approaches to the rapid contact transfer of DNA to secondary surfaces because the extent of release or transfer of DNA from the surfaces of coated balloons may no longer depend solely on the rate of film dissolution and the release of soluble DNA. We also reasoned that physical and mechanical forces that would be experienced either (i) during simple balloon inflation or (ii) when a film was pressed into firm and direct contact with other secondary surfaces upon balloon inflation (e.g., as would occur during inflation in an artery) might lead to more rapid, delamination and/or transfer of the films than was observed during the incubation of uninflated balloons in PBS buffer.

To test this hypothesis and characterize the inflation-mediated contact transfer of DNA to secondary surfaces under well-defined and controlled conditions, we developed a simple hydrogel hole-insertion model. For these experiments, we prepared thick slabs of agarose gel containing holes appropriately sized for the insertion and inflation of film-coated balloons (Scheme 1A). This agarose gel model is simple to prepare, and it enables parameters such as hole diameter and gel stiffness (as well as the extent of hydration, inflation time, and the balloon/hole ratio) to be varied in a soft, compliant, and transparent system that can be sliced and imaged readily to characterize the extent of film transfer using fluorescence microscopy. For the

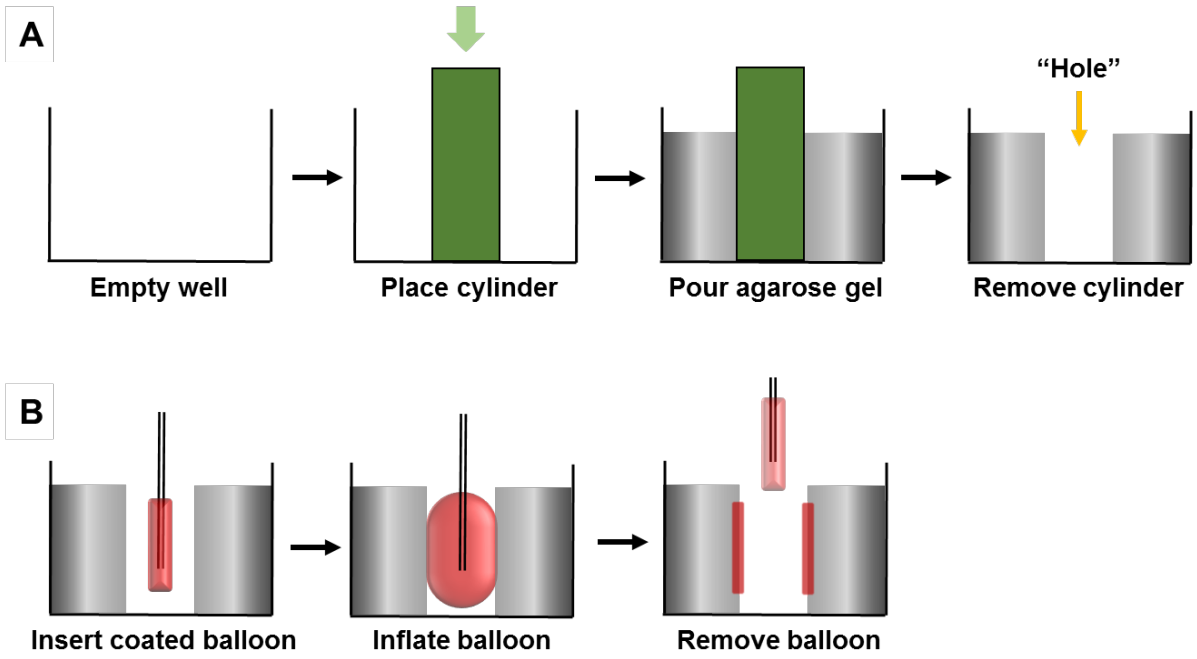

Scheme 1: (A) Schematic illustration showing the process used to design the agarose gel hole-insertion model used to characterize inflation-promoted contact transfer of DNA to soft surfaces. (B) Schematic illustration showing the insertion, inflation, and subsequent deflation and removal of a film-coated balloon using this gel model to characterize film transfer.

experiments described below, we prepared samples of 3% agarose (w/v) in PBS at pH 7.4.[65] A cylinder of known diameter was inserted during gel solidification and removed after the gel was completely solidified to create well-defined holes with sizes similar to those of arteries in rats and pigs (Scheme 1A; described in greater detail below).[40, 41] Characterization of the wet surfaces of the holes created using this method using pH paper revealed a pH of ~7.

Influence of Cavity Size on the Contact Transfer of DNA

In a first series of experiments using our hydrogel hole-insertion model, we sought to characterize the influence of the size of the hole on the contact transfer of DNA. Cylinders with different diameters of 2 mm, 3 mm, or 4 mm were used during the gel solidification stage to create gel slabs with holes 2 mm, 3 mm, or 4 mm in diameter. The panels in Figure 3A-D show a schematic illustration of a top-down view (Figure 3A) and three representative top-down optical microscopy views (Figure 3B-D) of gel slabs fabricated with holes with diameters of 2 mm, 3 mm, and 4 mm, respectively. The panels in Figure 3E-H show a schematic illustration of a side-view (Figure 3E) and three representative side-on optical microscopy images (Figure 3F-H) of the same gels shown in Figure 3B-D (the gels were sliced longitudinally along the long axis of the holes using a razor blade prior to imaging). Inspection of these images reveals well-defined holes with smooth edges.

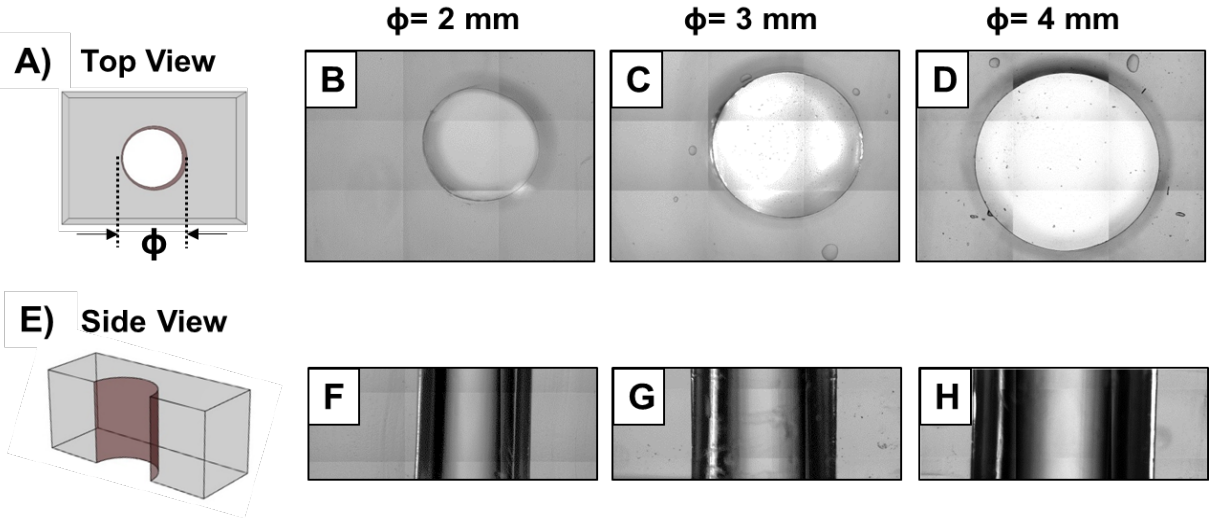

Figure 3: (A) Schematic illustration showing the top view of a gel slab containing a well-defined hole with diameter (Φ). (B-D) Representative top-down bright-field microscopy images of gel slabs with hole sizes of 2 mm (B), 3 mm (C) and 4 mm (D). (E) Schematic illustration showing a side view of a gel slab containing a well-defined hole. (F-H) Representative side-on bright-field microscopy images of gel slabs with hole sizes of 2 mm (F), 3 mm (G) and 4 mm (H).

Balloon catheters coated with $(LPEI/PAA/LPEI/DNA)_{32}$ films fabricated using fluorescently labeled DNA were then inserted into the holes in the gels and inflated for a predetermined duration (Scheme 1B). In this first series of experiments, film-coated balloons were inflated with 2 mL of air for two minutes, such that the surfaces of the balloons were pressed into firm contact with the edges of the holes. After deflation and removal of the balloon (Scheme 1B), the gel slab was imaged from both the top (Figure 4A-D) and the side (Figure 4E-K) as described above. Inspection of these images reveals bright red DNA-associated fluorescence distributed uniformly around the circumference of the holes in which the balloons were inflated. The linear red 'rays' observed to emanate from the surfaces of the holes in the top-down images in Figure 4B-D resulted from the transport of DNA into small cracks that formed in the gel during balloon inflation. Characterization of sliced gel slabs (Figure 4F-K) also revealed

that DNA was transferred to the gel along the length of the balloon (e.g., everywhere that the surface of the balloon was in contact with the gel during inflation). A comparison of the images in Figure 4I-K, which show bright-field images of side views of the gels after inflation of the balloons, to the images shown in Figure 3F-H before balloon inflation, also reveals the extent to which the surfaces of the holes are deformed during balloon inflation. Further evidence in support of the contact-transfer of DNA is shown in panels L-Q of Figure 4, which show images of the film-coated balloons before (Figure 4L-N) and after (Figure 4O-Q) the two minutes of inflation in the holes of the gel slabs used in these experiments. These images reveal decreases in the fluorescence intensities on the surfaces of the balloons after inflation, consistent with observations of the contact transfer of DNA to the surfaces of the holes in Figure 4B-D and 4F-H.

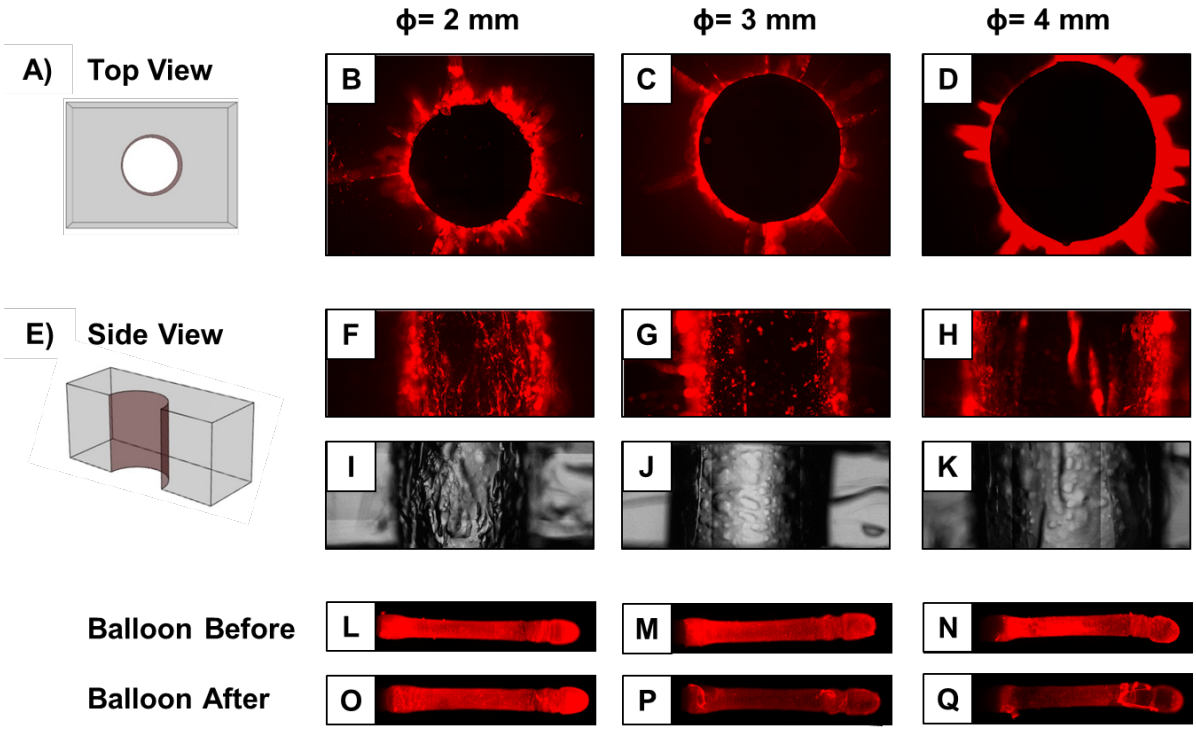

Figure 4: (A) Schematic illustration showing a top-down view of a gel slab containing a well-defined hole. (B-D) Representative top-down fluorescence microscopy images of gel slabs with hole sizes of 2 mm (B), 3 mm (C), and 4 mm (D) after the inflation of a film-coated balloon for two minutes. (E) Schematic illustration showing a side-on view of a gel slab containing a well-defined hole. (F-K) Representative side-on fluorescence microscopy (F-H) and bright-field (I-K) images of gel slabs with hole sizes of 2 mm (F,I), 3 mm (G,J), and 4 mm (H,K) after the inflation of a film-coated balloon for two minutes. (L-Q) Representative fluorescence microscopy images of film-coated balloons before (L-N) and after (O-Q) insertion in holes of size 2 mm (L,O), 3 mm (M,P), and 4 mm (N,Q) for two minutes.

To facilitate quantitative interpretations of these results, we measured the average fluorescence intensity on the surface of each film-coated balloon before (Figure 4L-N) and after (Figure 4O-Q) inflation in the hydrogel holes in the experiments described above, and then calculated the relative intensity of the DNA left on the balloons as the percentage of the original intensity prior to insertion and inflation (Figure 5). ANOVA Single Factor analysis of variance was used to determine the statistical significance of differences between each group with

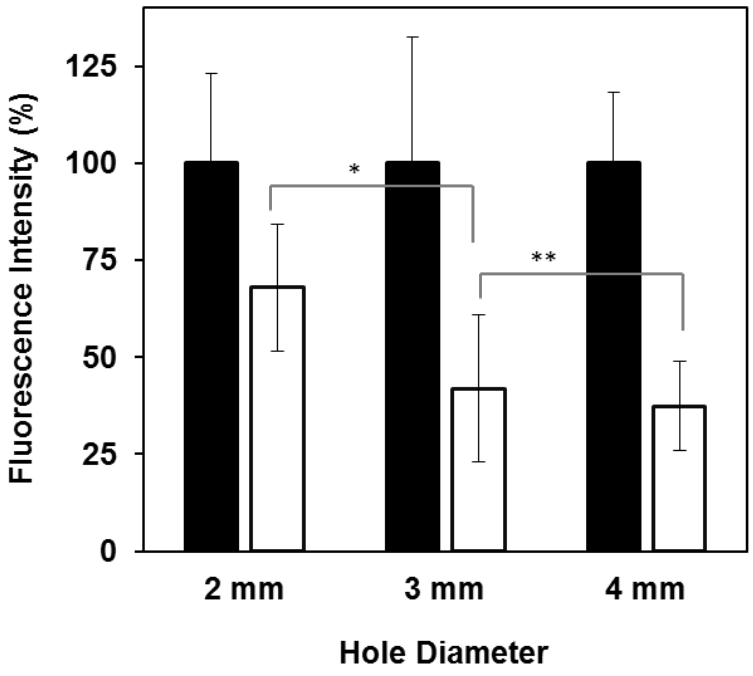

Figure 5: Plot showing the relative fluorescence intensities on the surfaces of film-coated balloons before and after insertion and inflation in gel slabs with hole sizes of 2 mm, 3 mm, and 4 mm. Average values and error bars (shown as standard deviations) were calculated using measurements for six arbitrarily chosen regions on the surfaces of the balloons shown in Figure 4L-Q (n = 6). The intensity values after balloon insertion (white bars) are presented as a percentage of the fluorescence intensity measured before balloon insertion (black bars). Statistical analyses were conducted using ANOVA Single Factor analysis of statistical variance with the following reported p values: *$p < 0.05$, **$p > 0.50$; N.S., non-significant.

different hole sizes. Inspection of this plot reveals that, for each hole diameter, there is a significant decrease ($p < 0.05$) in fluorescence intensity on the surface of each balloon (white bars) relative to the amount prior to insertion and inflation (black bars). In particular, only approximately 40% of the original amount of DNA remained on the surfaces of the balloons after two minutes of inflation in holes with sizes of 3 mm and 4 mm (corresponding to the contact transfer of approximately 60% of the DNA to the gel under these conditions).

Further analysis of the balloons used in these experiments demonstrated that, in general, the fluorescence remaining on the surfaces of film-coated balloons decreased as the diameter of the holes increased (differences between the fluorescence intensities on balloons inflated in 2 mm and either the 3 mm or 4 mm holes were determined to be statistically significant ($*p < 0.05$), while the difference between balloons inflated in 3 mm and 4 mm was not statistically significant ($**p > 0.50$). These results reveal the size of hole relative to the size of the balloon (and thus, likely, the extent to which the balloon and the coating are stretched upon inflation prior to making contact with the surface of the gel) to influence the extent of contact-mediated DNA transfer. For the remainder of the studies described below, we used gels containing holes 3 mm in diameter because this hole size led to significant amounts of contact transfer in this hydrogel model and it is more similar in size to the peripheral arteries of pigs used in our *in vivo* studies than the larger 4 mm holes.

Influence of Balloon Inflation Time on Contact Transfer of DNA

The results of the studies described above demonstrate that the inflation of film-coated balloons in a hydrogel containing a hole 3 mm in diameter leads to the contact transfer of ~60% of the DNA to the surface of the hole after insertion and inflation for two minutes. In a subsequent series of experiments, we sought to characterize the influence of balloon inflation time on the contact-transfer of DNA using this hydrogel hole-insertion model. For these studies, we performed experiments using gel slabs with holes 3 mm in diameter and three different short time durations of 5 minutes, 2 minutes, and 30 seconds. After deflation and removal of the balloons, the gel slabs were imaged from both the top (Figure 6A-D) and the side (Figure 6E-K)

using fluorescence microscopy. Inspection of these images again reveals bright red DNA-associated fluorescence distributed uniformly around the circumference of the holes (Figure 6A-D) and along the length of the hole that was in contact with the inflated balloon (Figure 6E-K). The images in Figure 6L-Q show the film-coated balloons imaged before (Figure 6L-N) and after (Figure 6O-Q) inflation in the holes of the gel slabs, revealing again a decrease in fluorescence intensity after deflation and removal and consistent with the levels of contact-transfer of DNA shown in Figure 6A-K.

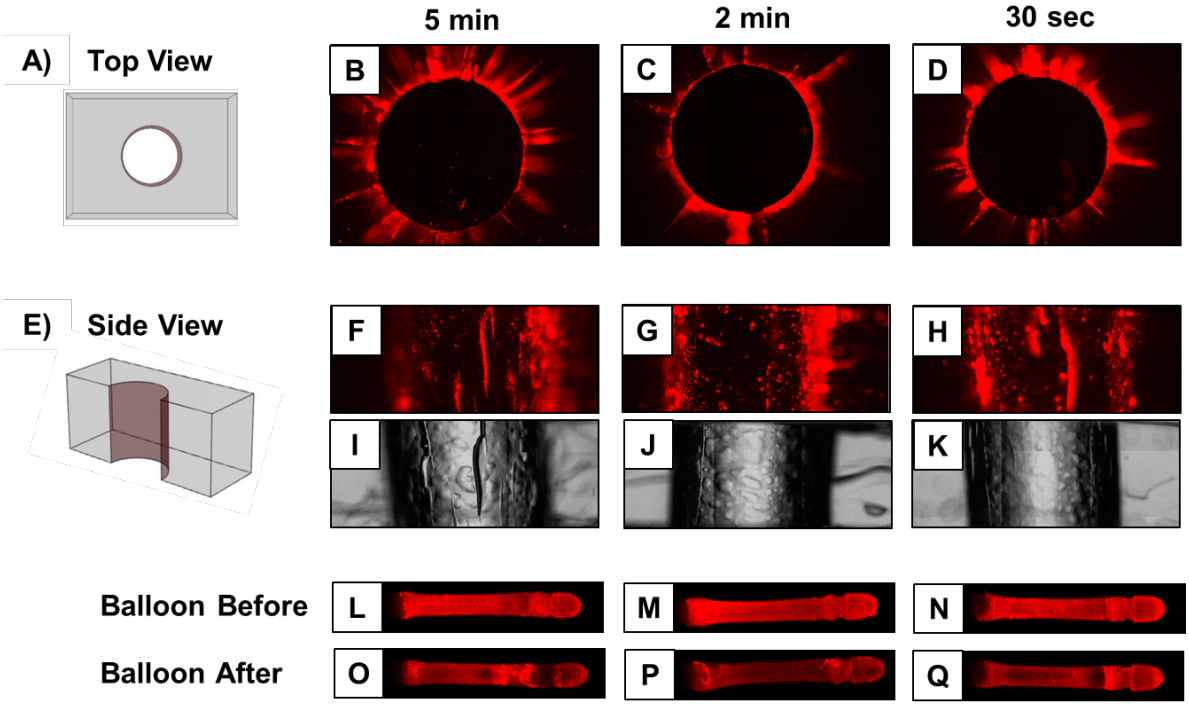

Figure 6: (A) Schematic illustration showing a top-down view of a gel slab containing a well-defined hole. (B-D) Representative top-down fluorescence microscopy images of gel slabs with a hole size of 3 mm after the inflation of a film-coated balloon for 5 min (B), 2 min (C), and 30 s (D). (E) Schematic illustration showing a side-on view of a gel slab containing a well-defined hole. (F-K) Representative side-on fluorescence microscopy (F-H) and bright-field (I-K) images of gel slabs with a hole size of 3 mm after the inflation of a film-coated balloon for 5 min (F,I), 2 min (G,J), and 30 s (H,K). (L-Q) Representative fluorescence microscopy images of film-coated balloons before (L-N) and after (O-Q) insertion in holes of size 3 mm for 5 min (L,O), 2 min (M,P), and 30 s (N, Q).

To quantify the amount of DNA transfer from the surface of each balloon, we again characterized the average fluorescence intensity on the surface of each film-coated balloon before (Figure 6L-N) and after (Figure 6O-Q) inflation in the hydrogel holes, and then calculated the relative intensity of the fluorescence on the balloons as the percentage of the original intensity prior to insertion and inflation (Figure 7). Inspection of this plot reveals a significant decrease in fluorescence intensity ($p < 0.05$) on the surface of each balloon after inflation (white

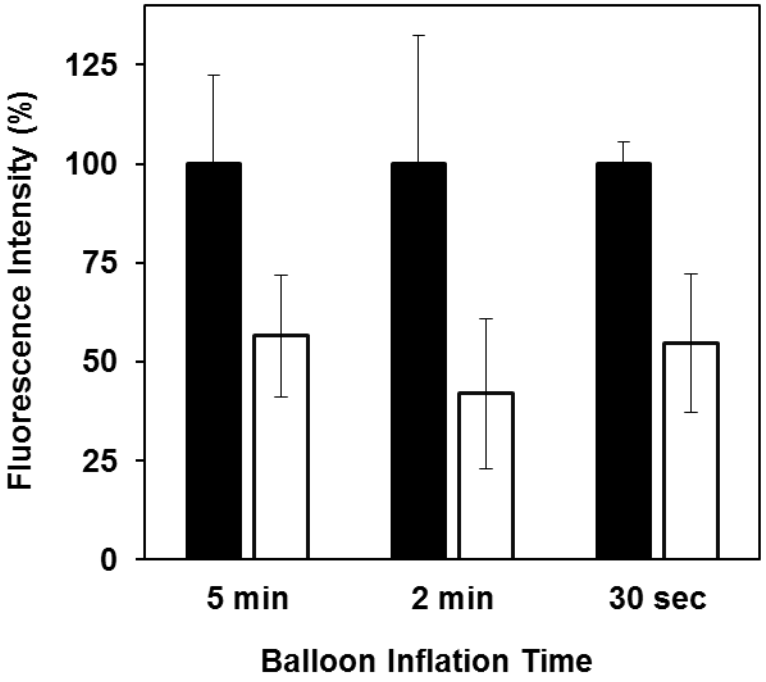

Figure 7: Plot showing the relative fluorescence intensities on the surfaces of film-coated balloons before and after insertion and inflation in gel slabs with a hole size of 3 mm for 5 min, 2 min, and 30 sec. Average values and error bars (shown as standard deviations) were calculated using measurements for six arbitrarily chosen regions on the surfaces of the balloons shown in Figure 6L-Q (n = 6). The intensity values after balloon insertion (white bars) are presented as a percentage of the fluorescence intensity measured before balloon insertion (black bars).

bars) relative to the amount present prior to inflation (black bars). Further analysis of balloons inflated at these three inflation times suggested no statistically significant differences between the amount of DNA transferred after 5 minutes, 2 minutes, or 30 seconds (with $p > 0.10$ for all comparisons).

It is not completely clear why longer inflation times do not lead to further increases in DNA transfer in this model, and why extents of transfer of ~60% appear to be the upper limit of the levels of contact transfer that can be achieved using this balloon/coating/hydrogel system.

We note that, because these experiments were conducted by inserting film-coated balloons into hydrogel holes devoid of bulk water (see Scheme 1B and Materials and Methods for additional details), and because the holes were not flushed with water prior to characterization by fluorescence microscopy, we regard the amounts of DNA that were contact-transferred to be equivalent to 100% of the initial amount of DNA minus the amount of DNA left on the balloons after deflation, since no other clear opportunities for the loss or removal of DNA from the system exist. One possibility is that while the top-most portion of the film may adhere strongly to the surface of the hydrogel (and thus remain transferred to the surface of the hole when the balloon is deflated and removed), the bottom-most portions of the coatings may adhere more strongly to the surface of the latex balloons used here. We note here, however, that in cases where the delamination of coatings was observed when film-coated balloons were incubated in PBS (Figure 2A), DNA was released or transferred into solution quantitatively. Because these hydrogel hole-insertion experiments were conducted using holes devoid of bulk water (Scheme 1B), this comparison hints at the role that the availability of abundant water may play in saturating or softening the films and/or influencing the nature of interactions at the balloon/coating interface in ways that lead to more effective or quantitative film transfer.

Overall, the results of these model experiments demonstrate that significant amounts of contact-transfer can be achieved by the inflation of films coated with $(LPEI/PAA/LPEI/DNA)_{32}$ for times as short as 30 seconds. In the studies described below, we selected the two shortest balloon inflation times investigated here (2 minutes and 30 seconds) to characterize the potential of this balloon-mediated approach to promote the rapid transfer of DNA to arterial tissue *in vivo*. The results of broader studies to exploit this and other hydrogel-based models to discover and

characterize the behaviors of other polyelectrolyte multilayer systems for the rapid contact transfer of DNA will be reported separately.[67]

Contact Transfer of DNA to Arterial Tissue in Rat and Pig Models of Arterial Injury

We demonstrated in a past study that balloon catheters coated with LPEI/PAA/LPEI/DNA films can be used to promote contact-transfer of DNA to vascular tissue using a rat model of carotid artery injury and a balloon inflation time of 20 minutes.[62] The conditions in that study were selected (i) on the basis of prior studies on the transfer of DNA using balloons coated with slowly-eroding hydrolytically degradable PEMs (also inserted and inflated for 20 minutes)[40, 41] and (ii) to maximize the likelihood of film transfer and local transgene expression in proof of concept experiments.

In the work reported here, we sought to characterize extents of balloon-mediated transfer of DNA to arterial tissue using substantially shorter inflation times of 2 minutes, 1 minute, or 30 seconds. These inflation times were selected, in part, based on the results of the studies described above using our agarose gel hole-insertion model. These times were also selected to evaluate extents of DNA transfer on clinically relevant time scales. For these experiments, we used two relevant animal models: (i) the rat model of carotid artery injury used in our past studies[40, 41] and (ii) a pig model to characterize the transfer of DNA to the femoral artery in a large animal model frequently used for the pre-clinical characterization of vascular interventions.[68] The panels in Figure 8A-C show schematic illustrations of the basic procedures used in these experiments. Unless otherwise noted, arterial tissue was harvested immediately after treatment with a film-coated balloon (i.e., after removal of the balloon, but prior to the restoration of blood flow) to

characterize extents of initial DNA transfer independent of any potential confounding effects of blood flow (see Materials and Methods for additional details related to surgical and tissue harvesting procedures).

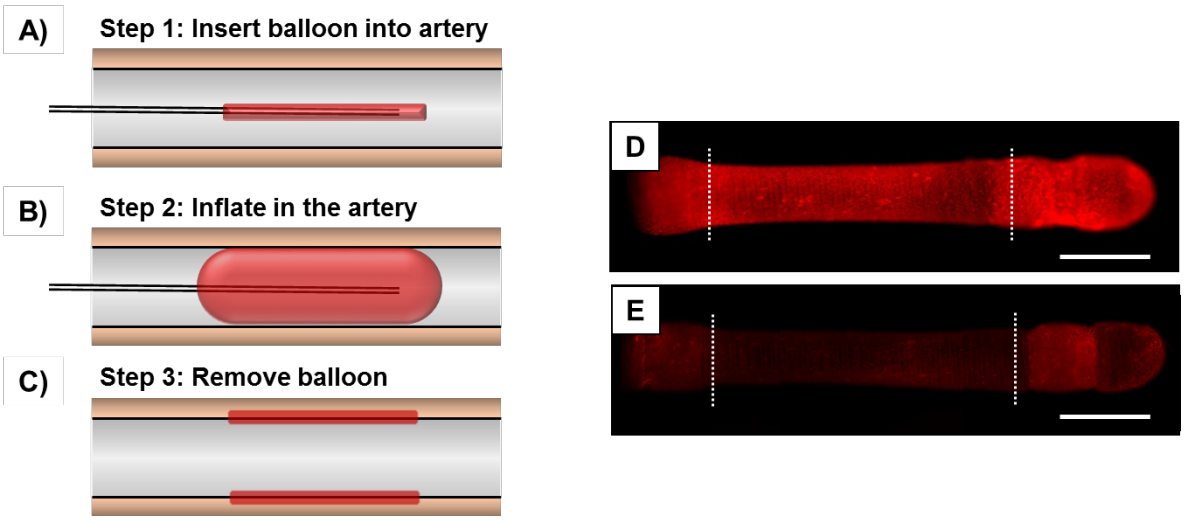

Figure 8: (A-C) Schematic illustration showing the insertion (A), inflation (B), and subsequent deflation and removal (C) of a film-coated balloon in an artery to promote the contact transfer of DNA to the arterial wall (C; shown in red). (D, E) Fluorescence microscopy images of a film-coated balloon before (D) and after (E) insertion and inflation in the artery of a pig for 30 sec (corresponding to results from experiments shown in Figure 10G-I; see text). Scale bars = 1 mm.

Figure 9 shows fluorescence microscopy images of cross-sections of rat carotid (Figure 9A-C) and pig femoral (Figure 9D-I) arteries after inflation of balloons coated with our $(LPEI/PAA/LPEI/DNA)_{32}$ quick-release films with inflation times of either 2 minutes (Figure 9A-C; rat model), 1 minute (Figure 9D-F; pig model), or 30 seconds (Figure 9G-I; pig model). All films were fabricated using DNA labeled with TMR, which appears in these images as red (the green in these images arises from tissue autofluorescence). Panels A, D, and G show a merge of images acquired through the red and green channels for each sample. Panels B, E, and H show corresponding images acquired through the red channel only (green tissue

autofluorescence not shown). The images in panels C, F, and I show higher magnification images acquired through the red channel showing additional details of the portions of panels B, E, and F enclosed by the dotted white squares.

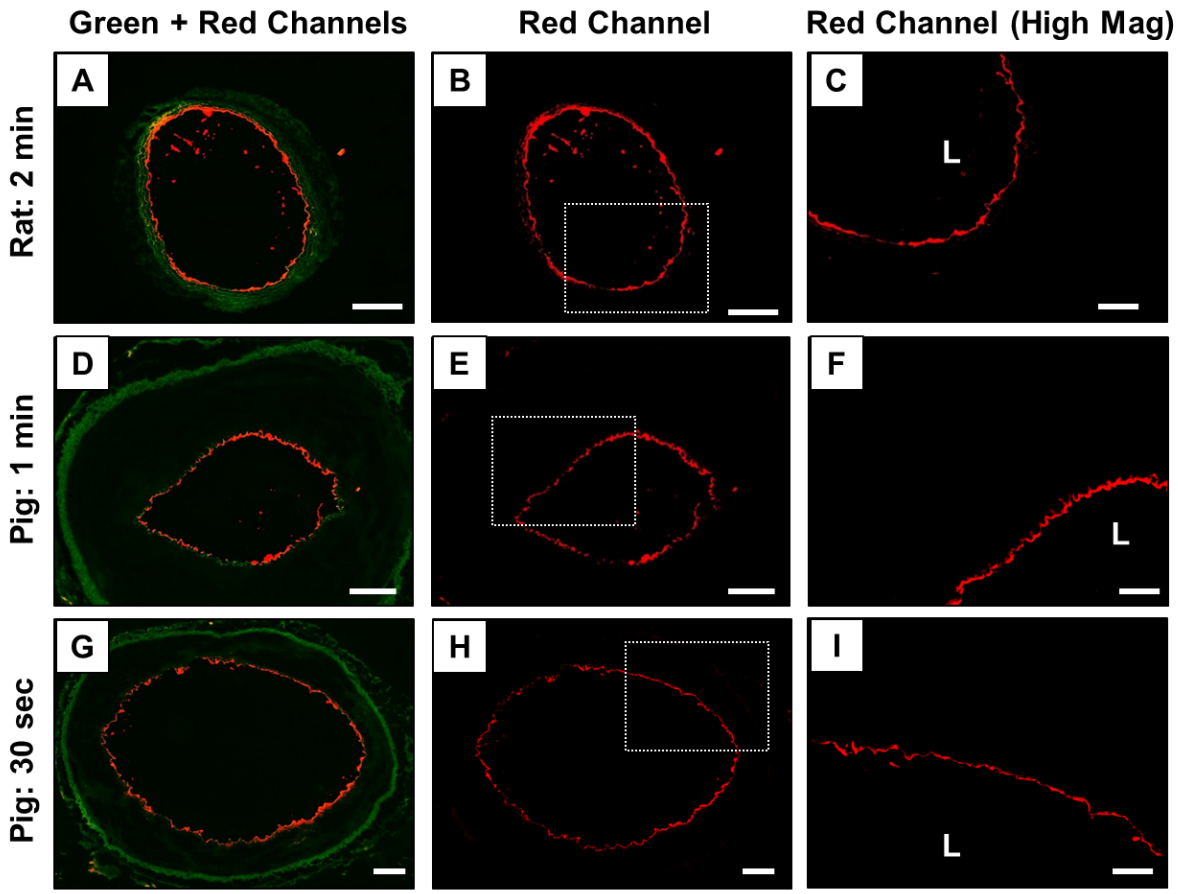

Figure 9: Fluorescence microscopy images showing the transfer of DNA to the arterial wall after the inflation of balloons coated with films fabricated using fluorescently labeled DNA in the carotid artery of a rat (A-C) or the femoral arteries of pigs (D-I) for either 2 minutes (A-C), 1 minute (D-F), or 30 seconds (G-I). Panels A, D, and G show a merge of images acquired through the red and green channels for each sample (red corresponds to DNA; green corresponds to tissue autofluorescence). Panels B, E, and H show corresponding images acquired through the red channel only. The images in panels C, F, and I show higher magnification images acquired through the red channel showing additional details of the portions of panels B, E, and F enclosed by the dotted white squares. The designation 'L' in images C, F, I indicates the location of the artery lumen. Scale bars for are 200 μm (A-B, D-E, G-H) and 100 μm (C,F,I) respectively.

Inspection of these images reveals the presence of bright red DNA-associated fluorescence located circumferentially along the luminal side of the arterial wall in each sample (e.g., at 2 minute, 1 minute, and 30 second inflation times). These results demonstrate that it is

possible to promote robust and uniform contact-transfer of DNA to vascular tissue in pigs using balloon inflation times as short as 30 seconds (Figure 9G-I) and in rats using times as short as 2 minutes, the shortest time tested in that species (Figure 9A-C). Fluorescence microscopy images of balloons before (Figure 8D) and after (Figure 8E) inflation and contact-transfer in pigs for 30 seconds also revealed a reduction in fluorescence consistent with the transfer of DNA from the surface of the balloon. The levels of reduction (~70%) observed here were generally greater than those described above (~60%) using the agarose gel insertion model. We speculate that differences in the physical, chemical, and mechanical properties and the more hydrated environment present in the blood vessels investigated here (relative to our hydrogel model) may contribute to promoting adhesion at the film/tissue interface and/or the disruption of adhesive interactions at the film/balloon interface. We note that while residual blood was present in the arteries at the time of insertion and inflation of the film coated balloons, the balloons were introduced within 1-2 centimeters of the treatment site in these experiments. The loss of DNA from the surfaces of the balloons is thus not likely to result from prolonged contact with blood prior to inflation and deployment at the treatment site, and the results shown in Figure 9 are consistent with the transfer of substantial amounts of DNA to the arterial wall under these conditions.

The results of these experiments are important for at least two reasons. First, they provide the basis of a new and useful approach to the rapid contact-transfer of DNA to vascular tissue in a clinically relevant large animal model used frequently for the pre-clinical evaluation of new vascular interventional procedures. Second, they demonstrate methods for the robust transfer of

DNA upon inflation and contact with soft tissue on clinically relevant time scales (e.g., as short as 30 seconds, the shortest time evaluated in these studies).

Characterization of Dissemination of DNA in Arterial Tissue Following Contact-Transfer

The results of the studies above show that inflatable balloon catheters coated with $(LPEI/PAA/LPEI/DNA)_{32}$ films can promote the initial transfer of DNA to the luminal wall when inflated in the femoral arteries of pigs. We note, in this context, that past studies from our group using balloons coated with hydrolytically degradable multilayers have demonstrated that DNA that transferred to the injured carotid arteries of rats can subsequently be transported deeper into the medial layers of tissue (over a period of 10-24 hours), and that this approach can lead to robust gene expression in rat models.[41] We also note that significant differences exist between the arteries of rats and the larger, thicker, and less mechanically compliant arteries of pigs.[68] We conducted a final experiment to characterize the extent to which this balloon-mediated approach to rapid DNA transfer might also promote the time-dependent dissemination of DNA deeper into the medial layer of tissue in the femoral arteries of pigs.

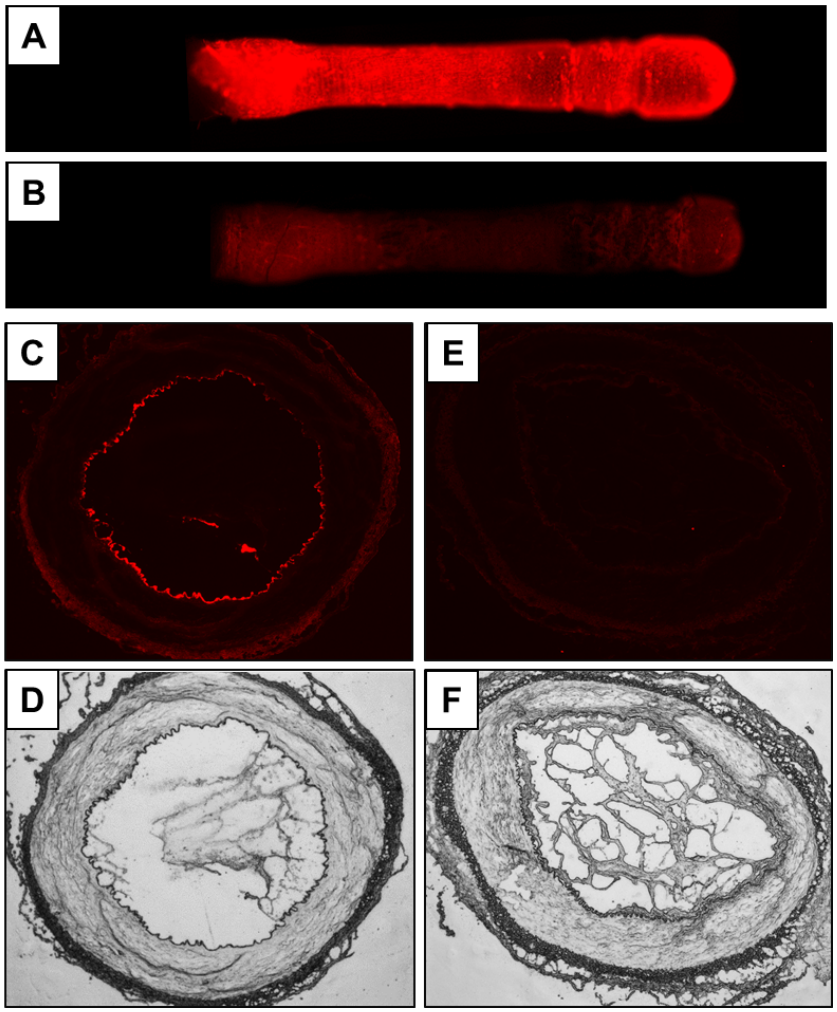

Figure 10: (A-B) Representative fluorescence microscopy images of a film-coated balloon before (A) and after (B) insertion in the femoral artery of a pig for one minute. (C-D) Representative fluorescence microscopy image (C) and the corresponding bright-field image (D) of a cross-section of an artery treated with the film-coated balloon shown in (A-B). (E-F) Representative fluorescence and bright-field microscopy images of an uninjured and untreated artery used as a control.

For these experiments, balloons coated with films fabricated using fluorescently labeled DNA were inserted into the femoral arteries of pigs and inflated for 1 minute to promote initial film transfer, as described in the section above. Figure 10 shows representative fluorescence microscopy images of a balloon used in these experiments before (Figure 10A) and after (Figure

10B) inflation and removal from the artery. Inspection of these images reveals a substantial decrease (~80%) in fluorescence intensity on the surface of the balloon, consistent with the results described above and confirming the transfer of DNA in this experiment. After removal of the balloon, blood flow was restored for 15 hours prior to the harvesting, processing, and imaging of the balloon-treated tissue.

Figure 10 also shows representative fluorescence and bright-field microscopy images of cross-sections of the artery treated with this film-coated balloon (Figure 10C-D) as well as images of an uninjured and untreated artery control (Figure 10E-F). Inspection of the image in Figure 10C reveals intense but variable levels of red, DNA-associated fluorescence on the luminal side of the artery. When compared to the result shown in Figure 10E (untreated control artery) this result demonstrates that significant amounts of DNA transferred during initial contact-transfer remain on the inner surface of the artery after 15 hours of exposure to normal blood flow (that is, DNA initially transferred is not completely rinsed or washed away upon the restoration of blood flow for at least 15 hours). It is possible that significant amounts of transferred DNA are also lost upon the restoration of blood flow, but the experiments described here did not address that question. The non-uniform distribution of red fluorescence in Figure 10C could result from non-uniform loss of DNA upon the restoration of blood flow or the non-uniform initial transfer of DNA during the contact-transfer procedure (or some combination of both factors; other possibilities are discussed below). Regardless, we conclude on the basis of these results that substantial amounts of DNA remain on the surface of the treated artery for 15 hours after blood flow is restored.

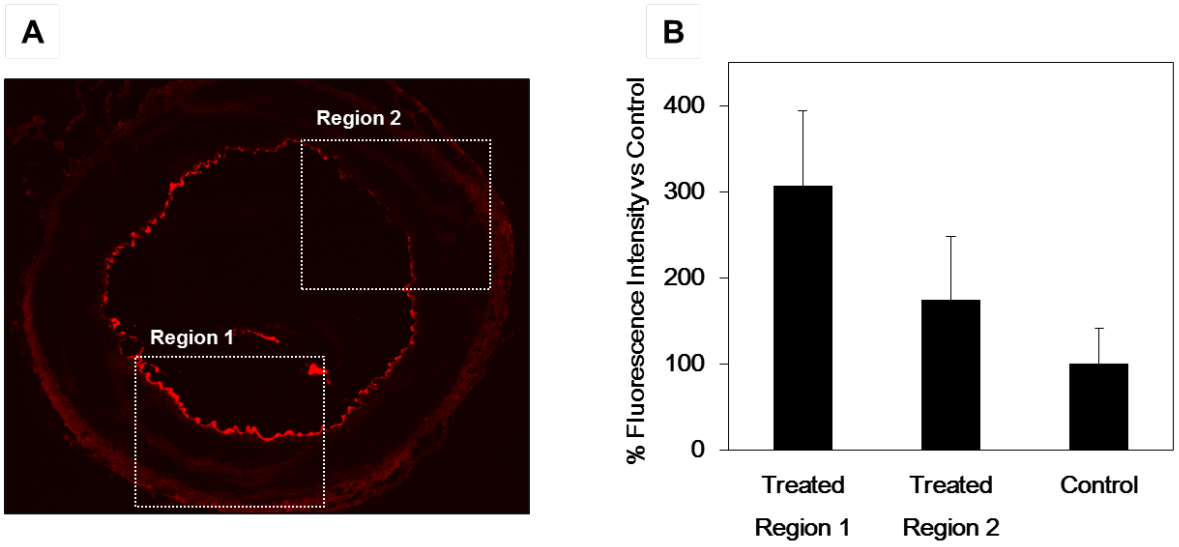

Figure 11: (A) Reproduction of the fluorescence microscopy image of the cross-section of the balloon-treated artery shown in Figure 10C, augmented with two boxed regions (1 and 2) enclosing two areas of high and low fluorescence intensity in the medial layer of the tissue. (B) Plot showing the relative fluorescence intensities in regions 1 and 2 compared to that of representative regions of the control artery shown in Figure 10E. Average values and error bars (shown as standard deviations) were calculated using measurements made in 10 arbitrarily chosen areas in regions 1 and 2 shown in (A). Statistical analyses were conducted using ANOVA Single Factor analysis of statistical variance with p (region 1, control), p (region 2, control) and p (region 1, region 2) < 0.05.

Further inspection and analysis of the image shown in Figure 10C reveals lower and non-uniform levels of fluorescence in the medial layers and around the circumference of the treated artery that appear to be higher than those observed in the medial layer of the untreated control artery (Figure 10E). This result suggests that DNA can potentially be transported from the luminal side of the arterial wall more deeply into medial tissue over the 15-hour period following initial transfer. To further characterize the extents of DNA dissemination in the media layers of arterial tissue arising from this experiment, we selected two regions in the medial layer of the treated artery of a pig (n=1) where high levels of fluorescence (Region 1, dashed box in Figure 11A) and low levels of fluorescence (Region 2, dashed box in Figure 11A) were observed

and quantified fluorescence intensities in these regions using computer image analysis. Average fluorescence intensities (with standard deviations) were calculated using measurements in 10 arbitrarily chosen areas in the medial layers of tissue located in Regions 1 and 2 of the image shown in Figure 11A. The results of this analysis are shown in the plot in Figure 11B. Statistical analysis conducted using ANOVA Single Factor analysis of statistical variance revealed the intensity of fluorescence in the medial layer in Region 1 to be significantly higher than that in the medial layer in Region 2 ($p < 0.05$), and the average fluorescence intensities in both Regions 1 and 2 were significantly higher ($p < 0.05$) than those measured in the medial layers of tissue in the uninjured and untreated control (e.g., Figure 10E).

These results are preliminary and arise from the analysis of tissue samples from a single biological replicate, but provide further support for the view that DNA that is initially transferred to the luminal side of the arterial wall of the femoral artery in pigs may also be transported deeper into medial tissue. They also suggest that the transport of DNA into the medial layer of tissue in Region 1 occurred to a greater extent than the transport of DNA into the medial layer of tissue in Region 2. This difference is likely a result of variability in the initial transfer of DNA to the portions of the luminal walls in these regions (as discussed above). In view of the results shown in Figure 11B, we consider the alternative possibility of the faster dissemination of uniformly-transferred DNA into medial tissue in Region 2 (as compared to Region 1) to be less likely. Such potential differences in non-uniform DNA dissemination and transport deeper into tissue could also result from non-uniformities in the extents of initial balloon-mediated arterial injury (e.g., prior to the balloon-treatment step; see Materials and Methods for details); additional experiments would be required to investigate that possibility more completely.

Summary and Conclusions

Our results demonstrate that polymer coatings assembled from LPEI, DNA, and PAA can promote balloon-mediated transfer of DNA to arterial tissue and other soft surfaces with balloon inflation times as short as 30 seconds. These times are substantially shorter than contact-transfer times of 20 minutes reported in past studies on thinner LPEI/PAA/DNA coatings. Studies of contact transfer in rat and pig models of peripheral arterial injury reveal inflation times of 30 seconds to one minute to promote circumferential transfer of fluorescently labeled DNA to the arterial wall, and suggest that transferred DNA is able to subsequently diffuse or be transported into medial layers of tissue in pigs over a period of 15 hours. The experiments described here were focused largely on understanding the time scales over which these materials can be used to promote the initial contact transfer of fluorescently labeled plasmid DNA. Follow-up studies using reporter plasmids will be necessary to understand relationships between inflation time, contact transfer, and extents of subsequent gene expression that can ultimately be achieved at these short inflation times. In addition to studies of the transfer of DNA to arterial tissue, we also developed a straightforward agarose gel-based hole-insertion model that can be used to characterize the contact-mediated transfer of DNA to other soft surfaces and probe parameters that influence contact transfer in this system. In addition to the potential utility of these materials in the context of gene delivery, the weak polyelectrolyte approach to promoting rapid release and contact transfer of DNA could also prove useful for the design of other types of ‘quick-release’ multilayers that promote rapid contact-transfer of siRNA, proteins, peptides, or other

biomolecules of interest in other fundamental or applied biomedical and biotechnological contexts.

Acknowledgments. Financial support was provided by the National Institutes of Health (R01 EB006820), the UW-Madison Office of the Vice Chancellor for Research and Graduate Education (VCRGE), and the National Science Foundation through a grant provided to the UW-Madison Materials Research Science and Engineering Center (MRSEC; DMR-1720415). The authors acknowledge use of instrumentation supported by the NSF through the UW MRSEC (DMR-1720415). V. A. was supported in part by a UW-Madison Morgridge Biotechnology fellowship and an American Heart Association (AHA) predoctoral fellowship. We thank Namrata Raman for assistance with SEM imaging, Jill Koch for assistance with animal surgeries, and Drew Roenneburg for assistance with the processing and sectioning of tissue samples.

ORCID

David M. Lynn: 0000-0002-3140-8637

References

(1) Decher, G.; Schlenoff, J. B. *Multilayer Thin Films: Sequential Assembly of Nanocomposite Materials*; Wiley-VCH: Weinheim, Germany, 2012; Vol. 1.

(2) Decher, G.; Schlenoff, J. B. *Multilayer thin films: sequential assembly of nanocomposite materials*; Wiley-VCH: Weinheim, Germany, 2012; Vol. 2.

(3) Picart, C.; Caruso, F.; Voegel, J.-C. *Layer-by-layer films for biomedical applications*; Wiley-VCH, 2015; Vol. 1.

(4) Decher, G. Fuzzy nanoassemblies: toward layered polymeric multicomposites. *Science* **1997**, *277*, 1232-1237.

(5) Boudou, T.; Crouzier, T.; Ren, K.; Blin, G.; Picart, C. Multiple Functionalities of Polyelectrolyte Multilayer Films: New Biomedical Applications. *Adv. Mater.* **2010**, *22*, 441-467.

(6) Borges, J.; Mano, J. F. Molecular Interactions Driving the Layer-by-Layer Assembly of Multilayers. *Chem. Rev.* **2014**, *114*, 8883-8942.

(7) Borges, J.; Rodrigues, L. C.; Reis, R. L.; Mano, J. F. Layer-by-Layer Assembly of Light-Responsive Polymeric Multilayer Systems. *Adv. Funct. Mater.* **2014**, *24*, 5624-5648.

(8) Richardson, J. J.; Cui, J.; Björnmalm, M.; Braunger, J. A.; Ejima, H.; Caruso, F. Innovation in Layer-by-Layer Assembly. *Chem. Rev.* **2016**, *116*, 14828-14867.

(9) Zeng, J.; Matsusaki, M. Layer-by-layer assembly of nanofilms to control cell functions. *Polym. Chem.* **2019**, *10*, 2960-2974.

(10) Ren, K.-F.; Hu, M.; Zhang, H.; Li, B.-C.; Lei, W.-X.; Chen, J.-Y.; Chang, H.; Wang, L.-M.; Ji, J. Layer-by-layer assembly as a robust method to construct extracellular matrix mimic surfaces to modulate cell behavior. *Progress in Polymer Science* **2019**, *92*, 1-34.

(11) Liu, T.; Wang, Y.; Zhong, W.; Li, B.; Mequanint, K.; Luo, G.; Xing, M. Biomedical Applications of Layer-by-Layer Self-Assembly for Cell Encapsulation: Current Status and Future Perspectives. *Adv. Healthcare Mater.* **2019**, *8*, e1800939.

(12) Yuan, W.; Weng, G.-M.; Lipton, J.; Li, C. M.; Van Tassel, P. R.; Taylor, A. D. Weak polyelectrolyte-based multilayers via layer-by-layer assembly: Approaches, properties, and applications. *Adv. Colloid Interface Sci.* **2020**, *282*, 102200.

(13) Alkekhia, D.; Hammond, P. T.; Shukla, A. Layer-by-Layer Biomaterials for Drug Delivery. *Annual Review of Biomedical Engineering* **2020**, *22*, 1-24.

(14) Zelikin, A. N. Drug Releasing Polymer Thin Films: New Era of Surface-Mediated Drug Delivery. *ACS Nano* **2010**, *4*, 2494-2509.

(15) Pavlukhina, S.; Sukhishvili, S. Polymer assemblies for controlled delivery of bioactive molecules from surfaces. *Adv. Drug Delivery Rev.* **2011**, *63*, 822-836.

(16) Hammond, P. T. Layer-by-layer approaches to staging medicine from surfaces. *AIChE Journal* **2015**, *61*, 1106-1117.

(17) Sarode, A.; Annapragada, A.; Guo, J.; Mitragotri, S. Layered self-assemblies for controlled drug delivery: A translational overview. *Biomaterials* **2020**, *242*, 119929.

(18) Hsu, B. B.; Hagerman, S. R.; Hammond, P. T. Rapid and efficient sprayed multilayer films for controlled drug delivery. *Journal of Applied Polymer Science* **2016**, *133*,

(19) Machillot, P.; Quintal, C.; Dalonneau, F.; Hermant, L.; Monnot, P.; Matthews, K.; Fitzpatrick, V.; Liu, J.; Pignot-Paintrand, I.; Picart, C. Automated Buildup of Biomimetic Films in Cell Culture Microplates for High-Throughput Screening of Cellular Behaviors. *Adv. Mater.* **2018**, *30*, 1801097.

(20) Koenig, O.; Neumann, B.; Schlensak, C.; Wendel, H. P.; Nolte, A. Hyaluronic acid/poly(ethylenimine) polyelectrolyte multilayer coatings for siRNA-mediated local gene silencing. *PLoS One* **2019**, *14*, e0212584.

(21) Boehnke, N.; Correa, S.; Hao, L.; Wang, W.; Straehla, J. P.; Bhatia, S. N.; Hammond, P. T. Theranostic Layer-by-Layer Nanoparticles for Simultaneous Tumor Detection and Gene Silencing. *Angew. Chem. Int. Ed.* **2020**, *59*, 2776-2783.

(22) Wang, S.; Battigelli, A.; Alkekhia, D.; Fairman, A.; Antoci, V.; Yang, W.; Moore, D.; Shukla, A. Controlled delivery of a protein tyrosine phosphatase inhibitor, SHP099, using cyclodextrin-mediated host–guest interactions in polyelectrolyte multilayer films for cancer therapy. *RSC Advances* **2020**, *10*, 20073-20082.

(23) Martin, J. R.; Howard, M. T.; Wang, S.; Berger, A. G.; Hammond, P. T. Oxidation-Responsive, Tunable Growth Factor Delivery from Polyelectrolyte-Coated Implants. *Adv. Healthcare Mater.* **2021**, *10*, e2001941.

(24) Chou, J. J.; Berger, A. G.; Jalili-Firoozinezhad, S.; Hammond, P. T. A design approach for layer-by-layer surface-mediated siRNA delivery. *Acta Biomater.* **2021**, *135*, 331-341.

(25) Rengaraj, A.; Bosc, L.; Machillot, P.; McGuckin, C.; Milet, C.; Forraz, N.; Paliard, P.; Barbier, D.; Picart, C. Engineering of a Microscale Niche for Pancreatic Tumor Cells Using Bioactive Film Coatings Combined with 3D-Architectured Scaffolds. *ACS Applied Materials & Interfaces* **2022**, *14*, 13107-13121.

(26) Jewell, C. M.; Lynn, D. M. Multilayered polyelectrolyte assemblies as platforms for the delivery of DNA and other nucleic acid-based therapeutics. *Adv. Drug Delivery Rev.* **2008**, *60*, 979-999.

(27) Wong, S. Y.; Moskowitz, J. S.; Veselinovic, J.; Rosario, R. A.; Timachova, K.; Blaisse, M. R.; Fuller, R. C.; Klibanov, A. M.; Hammond, P. T. Dual Functional Polyelectrolyte

Multilayer Coatings for Implants: Permanent Microbicidal Base with Controlled Release of Therapeutic Agents. *J. Am. Chem. Soc.* **2010**, *132*, 17840-17848.

(28) Hammond, P. T. Engineering materials layer-by-layer: Challenges and opportunities in multilayer assembly. *AIChE J.* **2011**, *57*, 2928-2940.

(29) Shah, N. J.; Macdonald, M. L.; Beben, Y. M.; Padera, R. F.; Samuel, R. E.; Hammond, P. T. Tunable dual growth factor delivery from polyelectrolyte multilayer films. *Biomaterials* **2011**, *32*, 6183-6193.

(30) Wohl, B. M.; Engbersen, J. F. J. Responsive layer-by-layer materials for drug delivery. *J. Controlled Release* **2012**, *158*, 2-14.

(31) Holmes, C.; Daoud, J.; Bagnaninchi, P. O.; Tabrizian, M. Polyelectrolyte Multilayer Coating of 3D Scaffolds Enhances Tissue Growth and Gene Delivery: Non-Invasive and Label-Free Assessment. *Adv. Healthcare Mater.* **2014**, *3*, 572-580.

(32) Ogier, J. LbL-Based Gene Delivery: Challenges and Promises. In *Layer-by-Layer Films for Biomedical Applications*, 2015; pp 195-206.

(33) Wu, C.; Li, J.; Wang, W.; Hammond, P. T. Rationally Designed Polycationic Carriers for Potent Polymeric siRNA-Mediated Gene Silencing. *ACS Nano* **2018**, *12*, 6504-6514.

(34) Correa, S.; Boehnke, N.; Deiss-Yehiely, E.; Hammond, P. T. Solution Conditions Tune and Optimize Loading of Therapeutic Polyelectrolytes into Layer-by-Layer Functionalized Liposomes. *ACS Nano* **2019**, *13*, 5623-5634.

(35) Chou, J. J.; Berger, A. G.; Jalili-Firoozinezhad, S.; Hammond, P. T. A design approach for layer-by-layer surface-mediated siRNA delivery. *Acta Biomaterialia* **2021**, *135*, 331-341.

(36) Zhang, S.; Vaida, J.; Parenti, J.; Lindsey, B. A.; Xing, M.; Li, B. Programmed Multidrug Delivery Based on Bio-Inspired Capsule-Integrated Nanocoatings for Infected Bone Defect Treatment. *ACS Appl. Mater. Interfaces* **2021**, *13*, 12454-12462.

(37) Zhang, J.; Chua, L. S.; Lynn, D. M. Multilayered Thin Films that Sustain the Release of Functional DNA under Physiological Conditions. *Langmuir* **2004**, *20*, 8015-8021.

(38) Jewell, C. M.; Zhang, J.; Fredin, N. J.; Lynn, D. M. Multilayered polyelectrolyte films promote the direct and localized delivery of DNA to cells. *J. Controlled Release* **2005**, *106*, 214-223.

(39) Liu, X.; Zhang, J.; Lynn, D. M. Ultrathin multilayered films that promote the release of two DNA constructs with separate and distinct release profiles. *Adv. Mater.* **2008**, *20*, 4148-4153.

(40) Saurer, E. M.; Yamanouchi, D.; Liu, B.; Lynn, D. M. Delivery of plasmid DNA to vascular tissue in vivo using catheter balloons coated with polyelectrolyte multilayers. *Biomaterials* **2011**, *32*, 610-618.

(41) Bechler, S. L.; Si, Y.; Yu, Y.; Ren, J.; Liu, B.; Lynn, D. M. Reduction of intimal hyperplasia in injured rat arteries promoted by catheter balloons coated with polyelectrolyte multilayers that contain plasmid DNA encoding PKCδ. *Biomaterials* **2013**, *34*, 226-236.

(42) Lynn, D. M. Polyelectrolyte Multilayer Coatings for the Release and Transfer of Plasmid DNA. In *Layer-by-Layer Films for Biomedical Applications*, Wiley-VCH Verlag GmbH & Co. KGaA, 2015; pp 171-194.

(43) Lvov, Y.; Decher, G.; Sukhorukov, G. Assembly of thin films by means of successive deposition of alternate layers of DNA and poly(allylamine). *Macromolecules* **1993**, *26*, 5396-5399.

(44) Ren, K.; Ji, J.; Shen, J. Construction and enzymatic degradation of multilayered poly-L-lysine/DNA films. *Biomaterials* **2006**, *27*, 1152-1159.

(45) Meng, F.; Hennink, W. E.; Zhong, Z. Reduction-sensitive polymers and bioconjugates for biomedical applications. *Biomaterials* **2009**, *30*, 2180-2198.

(46) Blacklock, J.; You, Y.-Z.; Zhou, Q.-H.; Mao, G.; Oupicky, D. Gene delivery in vitro and in vivo from bioreducible multilayered polyelectrolyte films of plasmid DNA. *Biomaterials* **2009**, *30*, 939-950.

(47) Blacklock, J.; Mao, G.; Oupický, D.; Möhwald, H. DNA Release Dynamics from Bioreducible Layer-by-Layer Films. *Langmuir* **2010**, *26*, 8597-8605.

(48) DeMuth, P. C.; Su, X.; Samuel, R. E.; Hammond, P. T.; Irvine, D. J. Nano-Layered Microneedles for Transcutaneous Delivery of Polymer Nanoparticles and Plasmid DNA. *Adv. Mater.* **2010**, *22*, 4851-4856.

(49) Chang, H.; Ren, K.-F.; Wang, J.-L.; Zhang, H.; Wang, B.-L.; Zheng, S.-M.; Zhou, Y.-Y.; Ji, J. Surface-mediated functional gene delivery: An effective strategy for enhancing competitiveness of endothelial cells over smooth muscle cells. *Biomaterials* **2013**, *34*, 3345-3354.

(50) DeMuth, P. C.; Min, Y.; Huang, B.; Kramer, J. A.; Miller, A. D.; Barouch, D. H.; Hammond, P. T.; Irvine, D. J. Polymer multilayer tattooing for enhanced DNA vaccination. *Nat. Mater.* **2013**, *12*, 367-376.

(51) Hujaya, S. D.; Marchioli, G.; Roelofs, K.; van Apeldoorn, A. A.; Moroni, L.; Karperien, M.; Paulusse, J. M. J.; Engbersen, J. F. J. Poly(amido amine)-based multilayered thin films on 2D and 3D supports for surface-mediated cell transfection. *J. Controlled Release* **2015**, *205*, 181-189.

(52) Zhang, H.; Ren, K.-F.; Chang, H.; Wang, J.-L.; Ji, J. Surface-mediated transfection of a pDNA vector encoding short hairpin RNA to downregulate TGF-β1 expression for the prevention of in-stent restenosis. *Biomaterials* **2017**, *116*, 95-105.

(53) Zhang, H.; Huang, J.-J.; Wang, J.; Hu, M.; Chen, X.-C.; Sun, W.; Ren, K.-F.; Ji, J. Surface-Mediated Stimuli-Responsive Gene Delivery Based on Breath Figure Film Combined with Matrix Metalloproteinase-Sensitive Hydrogel. *ACS Biomater. Sci. Eng.* **2019**, *5*, 6610-6616.

(54) Yao, L.; Weng, W.; Cheng, K.; Wang, L.; Dong, L.; Lin, J.; Sheng, K. Novel Platform for Surface-Mediated Gene Delivery Assisted with Visible-Light Illumination. *ACS Appl. Mater. Interfaces* **2020**, *12*, 17290-17301.

(55) Fu, J.-Y.; Lai, Y.-X.; Zheng, S.-S.; Wang, J.; Wang, Y.-X.; Ren, K.-F.; Yu, L.; Fu, G.-S.; Ji, J. Mir-22-incorporated polyelectrolyte coating prevents intima hyperplasia after balloon-induced vascular injury. *Biomaterials Sci.* **2022**,

(56) Lynn, D. M. A "Multilayered" Approach to the Delivery of DNA: Exploiting the Structure of Polyelectrolyte Multilayers to Promote Surface-Mediated Cell Transfection and Multi-Agent Delivery. *Multilayer Thin Films* **2012**, 731-748.

(57) Sun, B.; Lynn, D. M. Release of DNA from polyelectrolyte multilayers fabricated using 'charge-shifting' cationic polymers: Tunable temporal control and sequential, multi-agent release. *J. Controlled Release* **2010**, *148*, 91-100.

(58) Zou, Y.; Xie, L.; Carroll, S.; Muniz, M.; Gibson, H.; Wei, W.-Z.; Liu, H.; Mao, G. Layer-by-Layer Films with Bioreducible and Nonbioreducible Polycations for Sequential DNA Release. *Biomacromolecules* **2014**, *15*, 3965-3975.

(59) Peng, N.; Yu, H.; Wang, Z.; Zhang, Y.; Deng, K.; Li, J.; Lu, L.; Zou, T.; Liu, Y.; Huang, S. Dendrimer-grafted bioreducible polycation/DNA multilayered films with low cytotoxicity and high transfection ability. *Materials Science and Engineering: C* **2019**, *98*, 737-745.

(60) Flessner, R. M.; Yu, Y.; Lynn, D. M. Rapid release of plasmid DNA from polyelectrolyte multilayers: A weak poly(acid) approach. *Chem. Commun.* **2011**, *47*, 550-552.

(61) Aytar, B. S.; Prausnitz, M. R.; Lynn, D. M. Rapid release of plasmid DNA from surfaces coated with polyelectrolyte multilayers promoted by the application of electrochemical potentials. *ACS Appl. Mater. Interfaces* **2012**, *4*, 2726-2734.

(62) Yu, Y.; Si, Y.; Bechler, S. L.; Liu, B.; Lynn, D. M. Polymer Multilayers that Promote the Rapid Release and Contact Transfer of DNA. *Biomacromolecules* **2015**, *16*, 2998-3007.

(63) Park, J. S.; Cho, S. M.; Han, G. Y.; Sim, S. J.; Park, J.; Yoo, P. J. Phase Controllable Transfer Printing of Patterned Polyelectrolyte Multilayers. *Langmuir* **2009**, *25*, 2575-2581.

(64) Herron, M.; Schurr, M. J.; Murphy, C. J.; McAnulty, J. F.; Czuprynski, C. J.; Abbott, N. L. Interfacial Stacks of Polymeric Nanofilms on Soft Biological Surfaces that Release Multiple Agents. *ACS Appl. Mater. Interfaces* **2016**, *8*, 26541-26551.

(65) Zhang, D.; Das, D. B.; Rielly, C. D. Microneedle Assisted Micro-Particle Delivery from Gene Guns: Experiments Using Skin-Mimicking Agarose Gel. *J. Pharm. Sci.* **2014**, *103*, 613-627.

(66) Saurer, E. M.; Jewell, C. M.; Roenneburg, D. A.; Bechler, S. L.; Torrealba, J. R.; Hacker, T. A.; Lynn, D. M. Polyelectrolyte Multilayers Promote Stent-Mediated Delivery of DNA to Vascular Tissue. *Biomacromolecules* **2013**, *14*, 1696-1704.

(67) Appadoo, V.; Carter, M. C. D.; Jennings, J.; Guo, X.; Liu, B.; Hacker, T. A.; Lynn, D. M. Stimuli-Responsive Polymer Coatings for the Rapid and Tunable Contact Transfer of Plasmid DNA to Soft Surfaces. *Submitted* **2022**.

(68) Byrom, M. J.; Bannon, P. G.; White, G. H.; Ng, M. K. C. Animal models for the assessment of novel vascular conduits. *J. Vasc. Surg.* **2010**, *52*, 176-195.

For Table of Contents Use Only: